NACA RM A56G06

NACA

RESEARCH MEMORANDUM

AN EXPERIMENTAL INVESTIGATION AT MACH NUMBERS FROM 2.1 TO 3.0 OF CIRCULAR-INTERNAL-CONTRACTION INLETS WITH TRANSLATING CENTERBODIES

By Emmet A. Mossman and Frank A. Pfyl

Ames Aeronautical Laboratory
Moffett Field, Calif.

NATIONAL ADVISORY COMMITTEE
FOR AERONAUTICS

WASHINGTON

October 31, 1956
Declassified December 1, 1959

NACA RM A56G06

NATIONAL ADVISORY COMMITTEE FOR AERONAUTICS

RESEARCH MEMORANDUM

AN EXPERIMENTAL INVESTIGATION AT MACH NUMBERS FROM 2.1 TO 3.0 OF CIRCULAR-INTERNAL-CONTRACTION INLETS WITH TRANSLATING CENTERBODIES

By Emmet A. Mossman and Frank A. Pfyl

SUMMARY

The total-pressure recovery characteristics of three circular internal-compression inlets with translating centerbodies were measured at free-stream Mach numbers, M_∞, from 2.1 to 3.0 at 0° geometric angle of attack. Each of the inlets had the same ratio of the minimum area to the entrance area ($A_{min}/A_i = 0.390$) when the apex of the centerbody coincided with the leading edge of the annulus. The inlets were empirically designed for Mach numbers near 2.5 since the contraction ratio was made to correspond to the value for isentropic recovery at $M_\infty = 2.47$. The three inlets differed only in the shape of the internal compression contours.

The pressure recovery of circular internal-compression inlets was found to be as good as, or slightly better than single cone inlets up to a Mach number of 3.0, the Mach number limit of this investigation. Of the inlets investigated the pressure recovery for the inlet having surface contours composed of straight-line elements was the highest in the Mach number range from 2.2 to 2.7. With this inlet, the maximum average total-pressure ratio at the simulated compressor inlet station for M_∞ of 2.5 was 0.77. At Mach numbers from 2.7 to 3.0 the inlet having internal contours designed empirically to approximate a uniform longitudinal pressure gradient had the highest pressure recovery.

Surveys near the minimum area section of the straight-contoured inlet showed that the shock-wave system was efficient, a pressure recovery of 96 percent of free-stream total pressure at $M_\infty = 2.5$ being measured in the center region of the duct. These measurements showed large pressure losses near the centerbody and annulus surfaces. However, further downstream, at the simulated compressor station, the total-pressure variation measured by the rake was only ±2 percent of the average value for the Mach number range from 2.1 to 2.5.

INTRODUCTION

Several investigators (refs. 1, 2, and 3) have indicated that the high wave drag associated with external-compression inlets at Mach numbers greater than 2.0 can be virtually eliminated by employing internal compression of the induction air. References 1 and 2 also reported that a circular internal-compression inlet can attain a pressure recovery equal to single cone inlets having external compression at Mach numbers up to about 2.3. Use of a circular internal-compression inlet can result, therefore, in a net gain in propulsive force at Mach numbers up to 2.3.

The present tests were made to investigate at higher Mach numbers the pressure-recovery characteristics of three internal-compression inlets similar in shape to those reported in references 1 and 2. The three inlets differed only in the shape of the internal contours. The investigation was exploratory and only the pressure recovery at 0° geometric angle of attack was measured. Included in this report is a discussion of the considerations governing the design of this type of inlet.

SYMBOLS

A	area, sq in.
$\frac{A_{min}}{A_i}$	contraction ratio (the minimum internal area of the inlet divided by the inlet entrance area without centerbody)
D	inlet entrance diameter, in.
D_A	local internal diameter of annulus, in.
D_B	local diameter of centerbody, in.
M	Mach number
p_t	total pressure, lb/sq ft
X	longitudinal distance from inlet lip station (positive direction downstream), in.
$\frac{X}{D}$	longitudinal distance from the inlet lip station divided by inlet entrance diameter
y	radial distance from centerbody surface, in.

Subscripts

c	compressor entrance station
i	inlet station (lip leading-edge station)
∞	free-stream condition

DESIGN CONSIDERATIONS AND MODELS

A review of previous attempts to develop satisfactory internal-compression inlets and considerations of the general requirements for efficient air-induction systems led to the following general criteria that were used as a guide in the design of a new type of internal-compression inlet.

1. Attainment of low wave drag by keeping the inclination of the external surfaces low relative to the air stream

2. Utilization of multishock internal compression for high pressure recovery

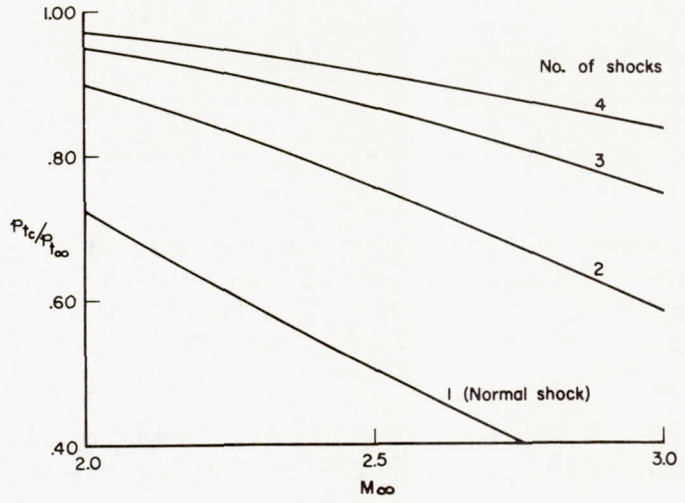
3. Avoidance of shock-induced separation during the internal-compression process

4. Elimination of corners in the internal duct

5. Use of a configuration in which the minimum area of the internal duct could be varied

The inclination of the external surfaces of an engine-inlet combination must be kept small if the wave drag of the combination is to be minimized. Theoretically, this can be achieved for a jet engine operating at Mach numbers above 2.0. At these speeds the diameter of the induction-air streamtube can be as large as the maximum diameter of the engine. Furthermore, an internal-compression inlet imposes no special requirements on the external shape of the engine-inlet combination. Thus, the external shape of the inlet-engine nacelle can be approximately cylindrical, making the angularity of the external surfaces small. It should be mentioned that, in contrast, inlets with external compression require large angularity of the external lip shape near the inlet entrance in order to secure maximum pressure recovery.

For high pressure recovery at Mach numbers above 2.0, multishock compression is necessary. The following sketch (for two-dimensional flow) shows that a single oblique-shock inlet (two-shock system) does not have a high theoretical pressure recovery. To increase the efficiency of

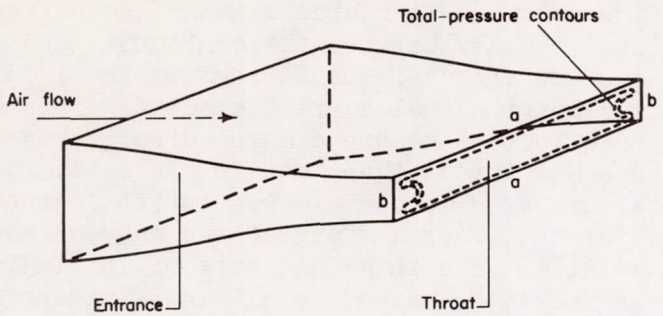


Sketch (a)

the compression process, two of the present inlets (inlets 1 and 2) have been designed to decelerate the induction air through a series of shock waves. In one instance (inlet 3) the internal contours have been shaped to attain shock-free (or isentropic) flow, that is, no coalescence of compression waves, in order to achieve efficient internal compression. (See ref. 4.)

Although the importance of shock-induced separation appears to have been recognized by early investigators in the field of air induction, prediction of its occurrence has not been possible due to the lack of adequate information on the pressure rise necessary to separate boundary layers at supersonic speeds. It is only through relatively recent research efforts that such information has been obtained (see refs. 5 and 6). In the design of the present internal compression inlets an attempt was made to minimize shock-induced separation by keeping the pressure rise across each shock wave low through small angularity of the compression surfaces and multishock compression. It should be remembered that, in addition to the step-like pressure increases due to shock waves, pressure gradients on axially symmetric compression surfaces will occur. The effect of the pressure gradient on the pressure ratios necessary for separation is, however, unknown.

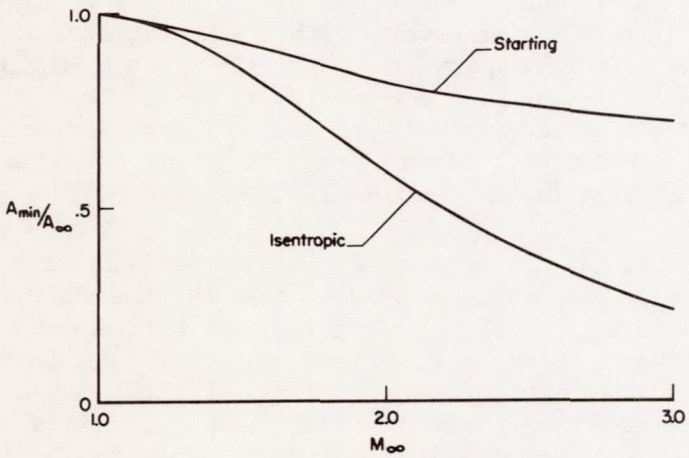
Where possible, corners should be eliminated in a ducting system because they can increase the pressure losses. Tests at supersonic speeds of rectangular inlets which have converging side walls, reference 7, showed the presence of concentrated regions of pressure loss in the minimum-area section. Sketch (b) illustrates that these pressure-loss



Sketch (b)

regions occurred at the sides b. Inlets with cross sections composed of circular elements should eliminate such local regions of high-pressure loss.

For an internal-compression inlet, efficient deceleration at any supersonic Mach number requires that the minimum area of the convergent-divergent duct be variable so that, first, the area can be large enough to permit establishment of supersonic flow in the converging portion of the duct and, second, the area can be reduced so that the ratio of minimum area to streamtube area can approach the isentropic value. The limits of the area-ratio variation are shown in the following sketch:



Sketch (c)

Three of the configurations evolved using the preceding design criteria are shown in the photograph of figure 1 and in the sketch of figure 2. A longitudinal cross section of inlet 1, shown in figure 2(a), indicates that the internal surface elements are straight lines. The annular and conical compression surfaces have small angularity, and the decrease in air-flow cross-section area between the entrance and the throat is apportioned equally between the centerbody and outer annulus when the apex of the centerbody is positioned at the leading edge of the annulus. The curved longitudinal surface elements of inlet 2 were empirically derived in an effort to secure a more uniform pressure gradient between the entrance and throat than that for inlet 1. One-dimensional flow relationships were used to compute the internal cross-sectional areas. Ordinates for the inner surface of the annulus and the centerbody are given in figure 2(b). The internal shape of inlet 3 was designed, using the method of characteristics, to eliminate strong shock waves. Ordinates and a sketch of this inlet are given in figure 2(c). For all three inlets the length of the annulus, the diameter of the inlet, and the minimum-contraction ratio are the same.

Provision was made to translate the centerbodies so that sufficient changes in the area ratio (A_{min}/A_i) could be attained to permit both starting and efficient compression at Mach numbers near 2.5. As the centerbody is moved forward, the ratio of the minimum area to the inlet area increases. Curves showing the longitudinal area distribution in terms of the ratio A_{local}/A_i for several positions of the centerbody are given for the three inlets in figures 3(a), (b), and (c). Figure 4 gives the area ratio, A_{min}/A_i, as a function of centerbody position. Study of these curves will show that for a given shape of the converging portion of the duct, the minimum area and its longitudinal location are functions of the shape of the rear portion of the centerbody. From consideration of efficient subsonic diffusion, the angle of this surface should be as small as possible. However, with small angles excessive translation of the centerbody is necessary to obtain the proper minimum area for starting. The present design is a compromise between these divergent requirements. (It should be noted that the use of long cylindrical sections on the centerbody for stabilization of the terminal shock wave also are prevented by the limitation on centerbody translation.)

When the apex of the centerbody was coincident with the lip leading edge, the ratio of the minimum area to the inlet area was 0.390 for each of the three inlets. This contraction ratio corresponds to the value for isentropic recovery at $M_\infty = 2.47$ (see sketch (c)). Because of the shock losses and boundary-layer growth on the centerbody and annulus, it is not possible to achieve isentropic recovery. The effect of these losses is to reduce the effective contraction ratio. Therefore, the inlets might be considered as designed for the Mach number range up to about 2.6.

APPARATUS AND PROCEDURE

The circular internal-compression inlets were tested in an 8- by 8-inch supersonic wind tunnel. A photograph of the wind tunnel with one of the models mounted in the test section is shown in figure 5. This wind tunnel is an intermittent-operation, nonreturn, variable-pressure wind tunnel equipped with an asymmetric sliding-block nozzle for varying the test-section Mach number. The dry-air supply, stored in five 36-foot-diameter pressure tanks at a maximum pressure of 150 pounds per square inch gauge, was of sufficient volume that data for a given Mach number and centerbody position could be obtained in a single run at nearly constant stagnation pressure. Tests were performed at Mach numbers from 2.1 to 3.0 at 0° geometric angle of attack and Reynolds numbers of approximately 10×10^{6} to 14×10^{6} per foot, respectively.

A sketch showing the details of the model mounting and instrumentation is given in figure 6. The centerbody, attached to the simulated compressor hub, was translated mechanically through a system of gears from outside the tunnel wall. The movable plug at the model base was likewise operated mechanically from outside the tunnel wall. The model was instrumented with 20 total-pressure tubes and 4 static-pressure tubes at the compressor inlet station (see fig. 6) to obtain the total- and static-pressure distribution. In addition to the pressure rakes at the compressor inlet, a few tests were performed with a static-pressure orifice and a total-pressure rake located 5-15/16 inches from the lip leading edge of inlet 1. The static-pressure orifice was placed in the annulus, and a hole through the annulus wall was provided so that a total-pressure rake could be translated vertically between the surfaces of the annulus and centerbody.

To insure that the boundary layer on the internal surfaces of the inlet would be turbulent, transition was fixed with small grooves near the lip leading edge and the tip of the centerbody for each configuration (see fig. 2). The size and number of grooves necessary to fix transition and still maintain a thin turbulent boundary layer were determined from the results of shadowgraph observations obtained from tests conducted in the Ames supersonic free-flight wind tunnel. Various centerbody positions were investigated for each model, and data were obtained only at plug positions for which the inlet would operate supercritically. The highest pressure recovery for each centerbody position at which the inlet would operate supercritically was taken as the maximum pressure recovery.

RESULTS

The pressure recovery measured for the three internal-compression inlets during the present investigation was a function of three variables; namely, free-stream Mach number, centerbody position, and location of the terminal shock wave inside the duct. (The inlets were designed to have the oblique wave from the center body apex fall inside the annulus lip leading edge so that the mass-flow ratio would be unity. However, this condition was not attained in the tests where inlets 1 and 3 operated below mass-flow ratios of unity at Mach numbers up to 2.3 and inlet 2 up to 2.7. For these conditions then, the inlets operated with various amounts of critical spillage which could effect slightly the external wave drag.) The pressure recovery increased with forward movement of the terminal shock wave to the most forward stable location; further forward movement of the wave resulted in a regurgitation of the wave and a reduction in the pressure recovery. (During the test, the terminal shock-wave position was set by the position of the plug at the exit.) The pressure recovery obtained with the shock wave in the most forward stable location is shown in figure 7 as a function of Mach number and contraction ratio. From these data the maximum pressure recovery for a constant Mach number was obtained and is presented for each of the inlets in figure 8 together with the corresponding contraction ratio.

The results of a total-pressure survey made near the minimum area section of inlet 1 ($X/D = 2.38$) are shown in figure 9. Surveys were made for free-stream Mach numbers of 2.1 and 2.5 with the inlet terminal shock wave ahead of and behind the survey station. Representative contour maps showing the total-pressure-recovery variations at the compressor inlet station are presented in figure 10 for inlet 1 at each Mach number tested and at the contraction ratio (or centerbody position) where the maximum pressure recovery was obtained.

DISCUSSION

The maximum pressure recoveries of the three circular internal-compression inlets of this investigation and the two similar circular inlets reported in reference 1 are compared in figure 8 with the best pressure recovery that has been obtained with single-cone inlets (see refs. 1 and 2). This figure shows the pressure recovery of circular internal-compression inlets to be as good as, or slightly better than, single-cone inlets up to a Mach number of 3.0, the limit of this investigation. It should be remembered that this recovery is achieved by the internal-compression inlets with comparatively low wave drag.

Inlet 1, which has compression surfaces generated by straight lines, had the highest recovery for the Mach number range from 2.2 to 2.7. Pressure recovery for inlet 2 was greater than that of the straight contoured

inlet at Mach numbers above 2.7. The inlet whose contours were derived using the method of characteristics, inlet 3, had the lowest pressure recovery. For inlet 3, theoretical calculations indicated a steep pressure gradient in the region near the minimum area, and it is possible that such gradients might have caused severe separation of the boundary layer.

For each of the inlets investigated the pressure recovery as a function of contraction ratio (or centerbody position) indicates that $\left(p_{t_c}/p_{t_\infty}\right)_{max}$ occurs near to, but is not always coincident with, the minimum value of the contraction ratio for supercritical operation (see fig. 7). Visual schlieren observation showed stable inlet flow during supercritical operation; that is, the internal shock system did not regurgitate.

Since inlet 1 had good pressure-recovery characteristics over a range of Mach numbers, additional pressure surveys were made to investigate the air flow in the region of the minimum area station. The internal shock-wave system produced efficient supersonic compression of the induction air. Total-pressure-recovery profiles measured at X/D = 2.38 (fig. 9) showed very high pressure recovery (p_t/p_{t_∞} = 0.97 at M_∞ = 2.1; p_t/p_{t_∞} = 0.96 at M_∞ = 2.5) in the center of the annular duct. The pressure losses were greatest near the centerbody and annulus surfaces, as would be expected. Further downstream at the simulated compressor inlet, the internal flow became sufficiently mixed that the total-pressure recovery contours (fig. 10) indicated only a slight deviation of about ±0.02 from the integrated mean pressure for the Mach number range from 2.1 to 2.5. Some asymmetry can be observed at the higher Mach numbers, which is attributed to the model being at an effective 1° to 1.5° angle of attack due to the wind-tunnel stream angle. The contours presented in figure 10 correspond to operation of the inlet near the maximum recovery at a given Mach number.

CONCLUSIONS

The following conclusions were obtained from an investigation at Mach numbers from 2.1 to 3.0 and a geometric angle of attack of 0° of three circular internal-compression inlets:

1. The pressure recovery of circular internal-compression inlets was as good as, or slightly better than, single cone inlets up to a Mach number of 3.0, the limit of this investigation.

2. The inlet which had compression surface contours composed of straight-line elements gave the highest pressure recovery over the Mach number range from 2.2 to 2.7.

3. The inlet which had internal contours designed empirically to approach a uniform longitudinal pressure gradient had the highest pressure recovery at Mach numbers from 2.7 to 3.0.

4. Very high pressure recovery (equal to 0.96 at a free-stream Mach number of 2.5) was measured in the center region of the duct near the minimum area of the inlet composed of straight-line elements.

5. The variation of total pressure at the compressor inlet station of the inlet with straight-line elements was ±2 percent for the Mach number range from 2.1 to 2.5.

Ames Aeronautical Laboratory
National Advisory Committee for Aeronautics
Moffett Field, Calif., July 6, 1956

REFERENCES

1. Mossman, Emmet A., and Pfyl, Frank A.: A Study of a Symmetrical, Circular, Internal Compression Inlet. NACA RM A55L16, 1956.

2. Mossman, Emmet A., Pfyl, Frank A., and Lazzeroni, Frank A.: Fuselage Side Inlets - A Study of Some Factors Affecting Their Performance and a Comparison With Nose Inlets. NACA RM A55F29, 1956.

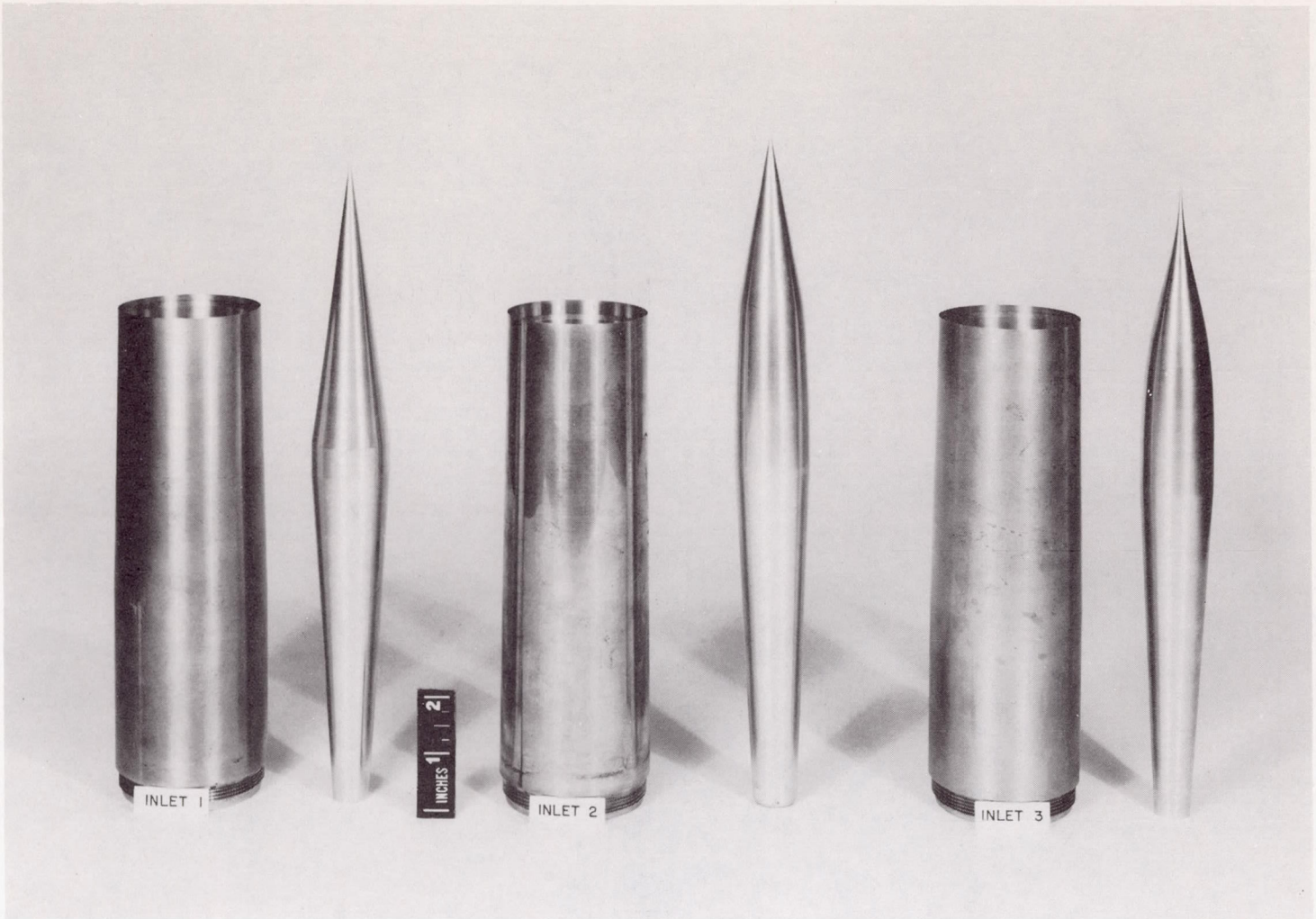
3. Ferri, Antonio, and Nucci, Louis M.: Theoretical and Experimental Analysis of Low-Drag Supersonic Inlets Having a Circular Cross Section and a Central Body at Mach Numbers of 3.30, 2.75, and 2.45. NACA RM L8H13, 1948.

4. Ferri, Antonio: Application of the Method of Characteristics to Supersonic Rotational Flow. NACA Rep. 841, 1946.

5. Chapman, Dean R., Kuehn, Donald M., and Larson, Howard K.: Preliminary Report on a Study of Separated Flows in Supersonic and Subsonic Streams. NACA RM A55L14, 1956.

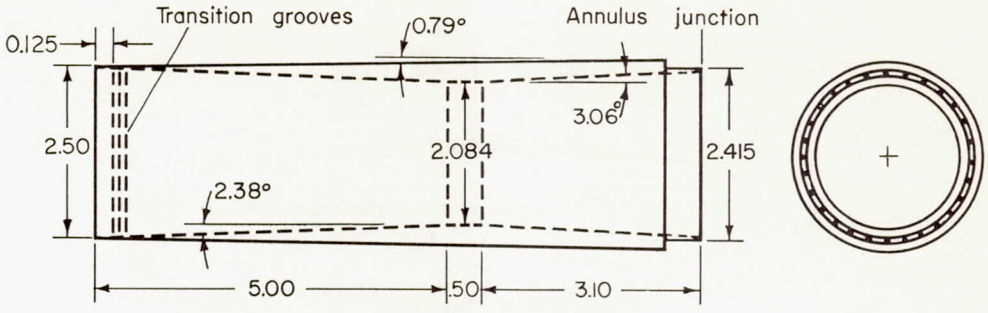
6. Bogdonoff, Seymour M.: Some Experimental Studies of the Separation of Supersonic Turbulent Boundary Layers. Rep. 336, Princeton Univ., Dept. Aero. Engr., June 1955.

7. Gunther, Fred: Development of a Two-Dimensional Adjustable Supersonic Inlet. Calif. Inst. of Tech., Jet Propulsion Lab. Rep. 20-247, Nov. 20, 1954.



A-21328

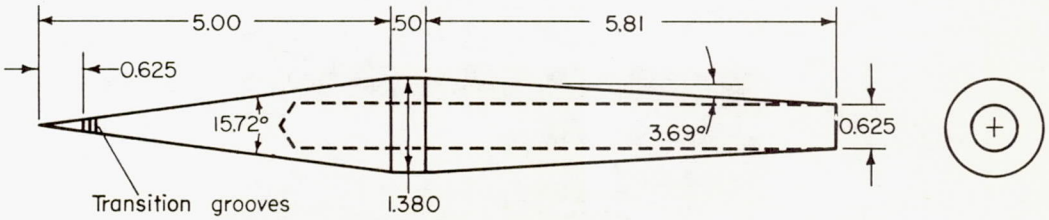
Figure 1.- Photograph of the circular internal-compression inlets.



Annulus

All dimensions in inches unless otherwise noted.

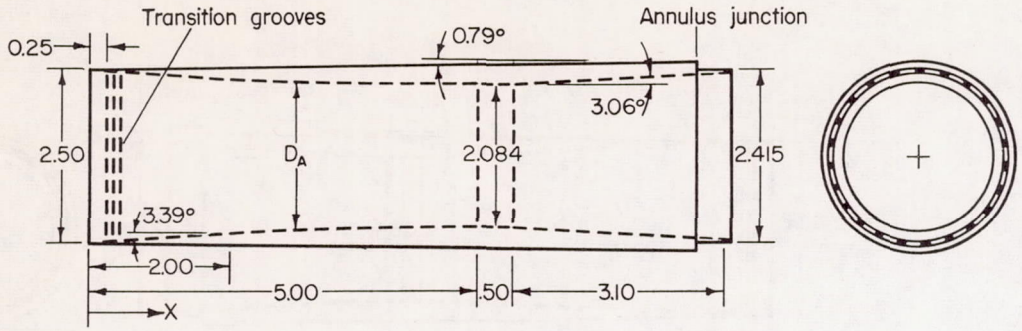
Note: Transition grooves consist of 6 grooves 0.003 deep by a 136° tool at 14.9 threads per inch.



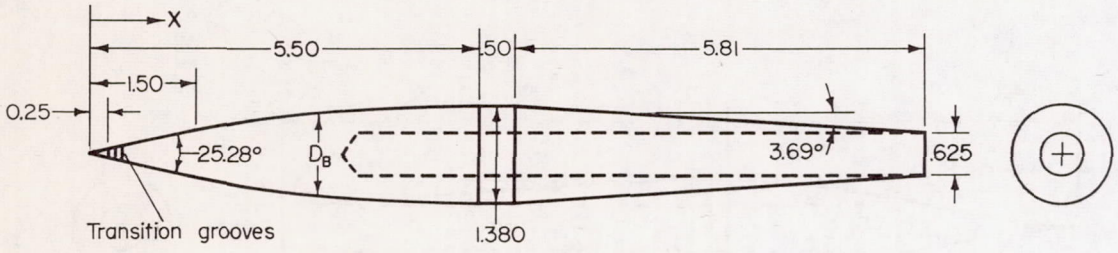
Centerbody

(a) Inlet I

Figure 2.- Sketch of annulus and centerbody details of the three inlet configurations.



Annulus



Centerbody

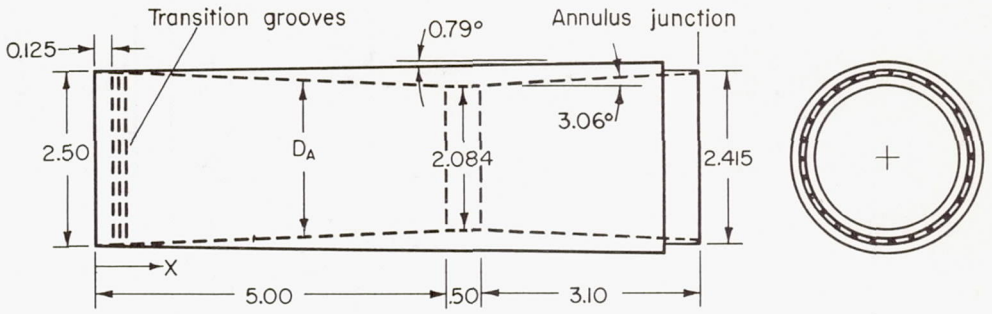
All dimensions in inches unless otherwise noted.

Coordinates of centerbody and annulus

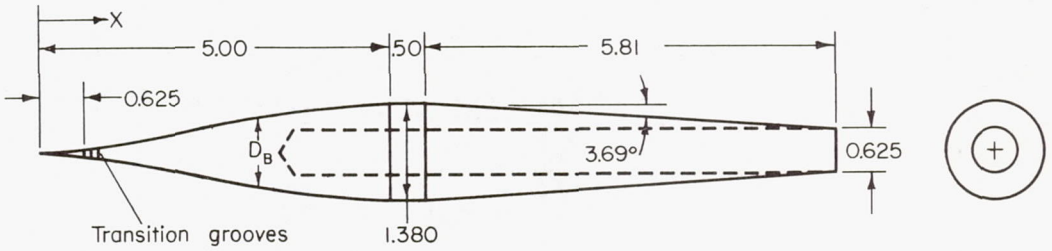
X	0	1.5	2.0	2.5	3.0	3.5	4.0	4.5	5.0	5.5
D_A	2.500	——	2.263	2.209	2.167	2.132	2.110	2.095	2.084	2.084
D_B	0	.671	.894	1.062	1.170	1.246	1.309	1.342	1.365	1.380

(b) Inlet 2

Figure 2.- Continued.



Annulus



Centerbody

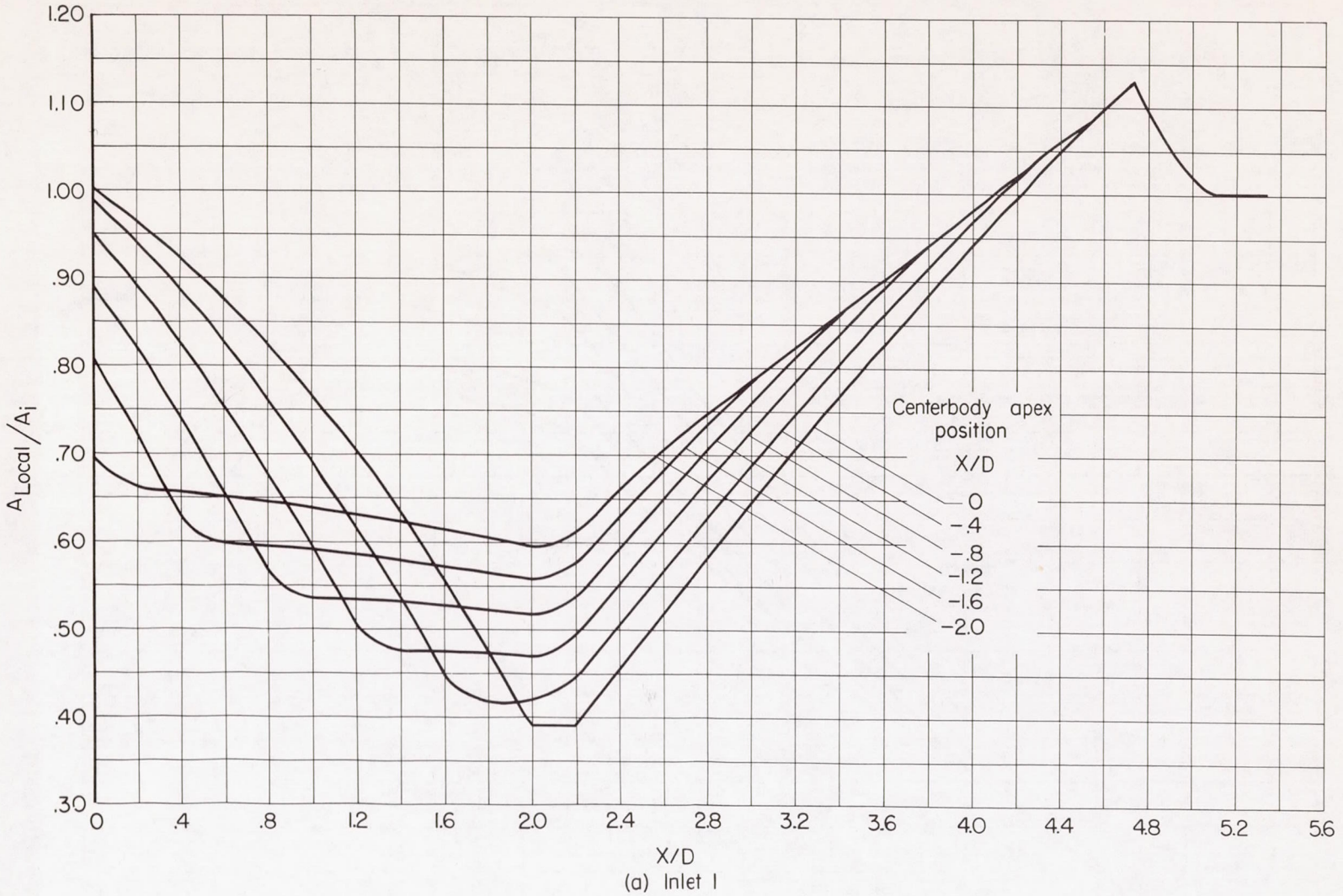
All dimensions in inches
unless otherwise noted.

Coordinates of centerbody and annulus

X	0	.5	1.0	1.5	2.0	2.5	3.0	3.5	4.0	4.5	5.0
D_A	2.500	2.480	2.466	2.448	2.416	2.362	2.294	2.212	2.142	2.100	2.084
D_B	0	.050	.156	.350	.600	.866	1.080	1.226	1.316	1.366	1.380

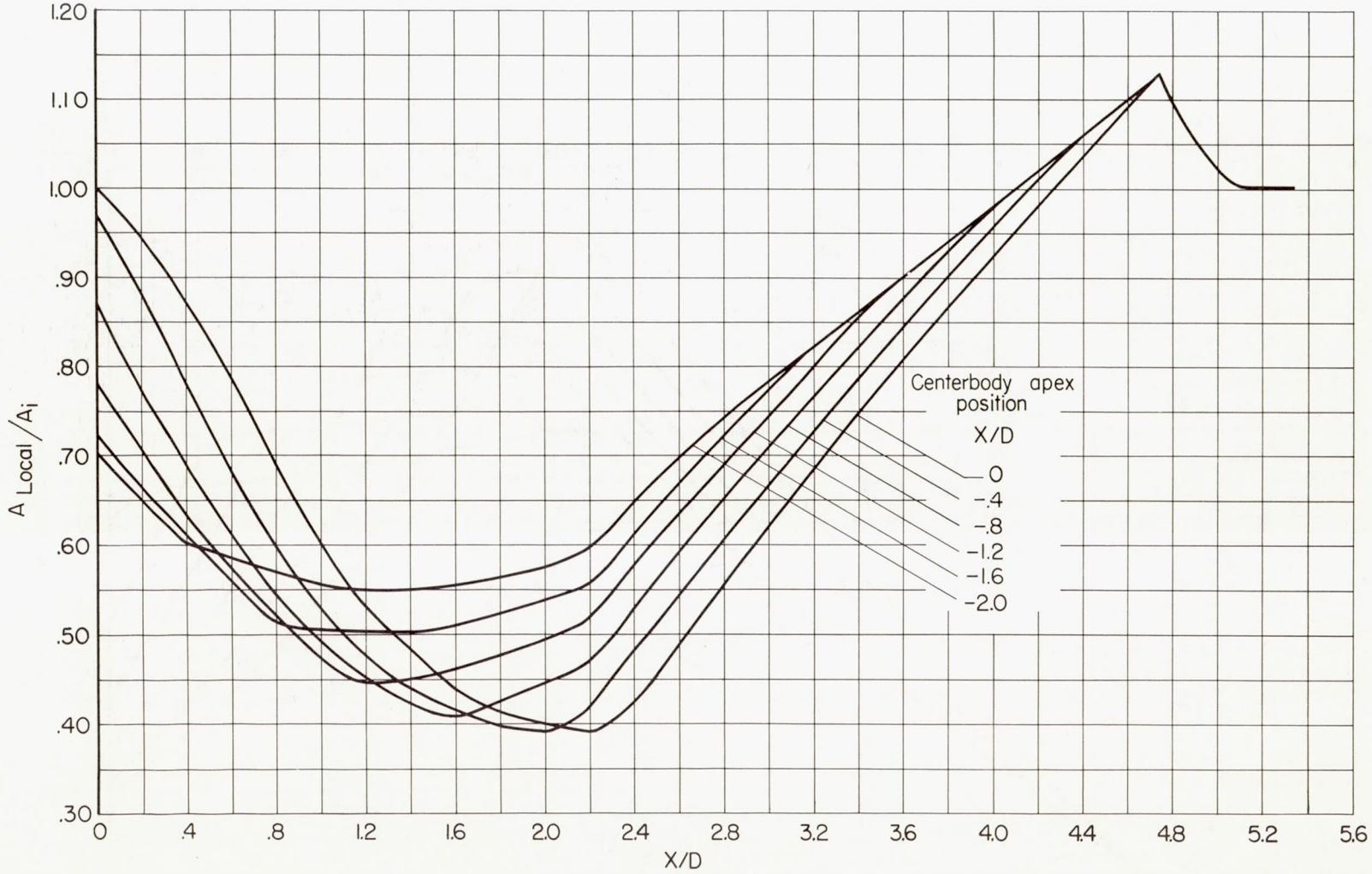
(c) Inlet 3

Figure 2.- Concluded.



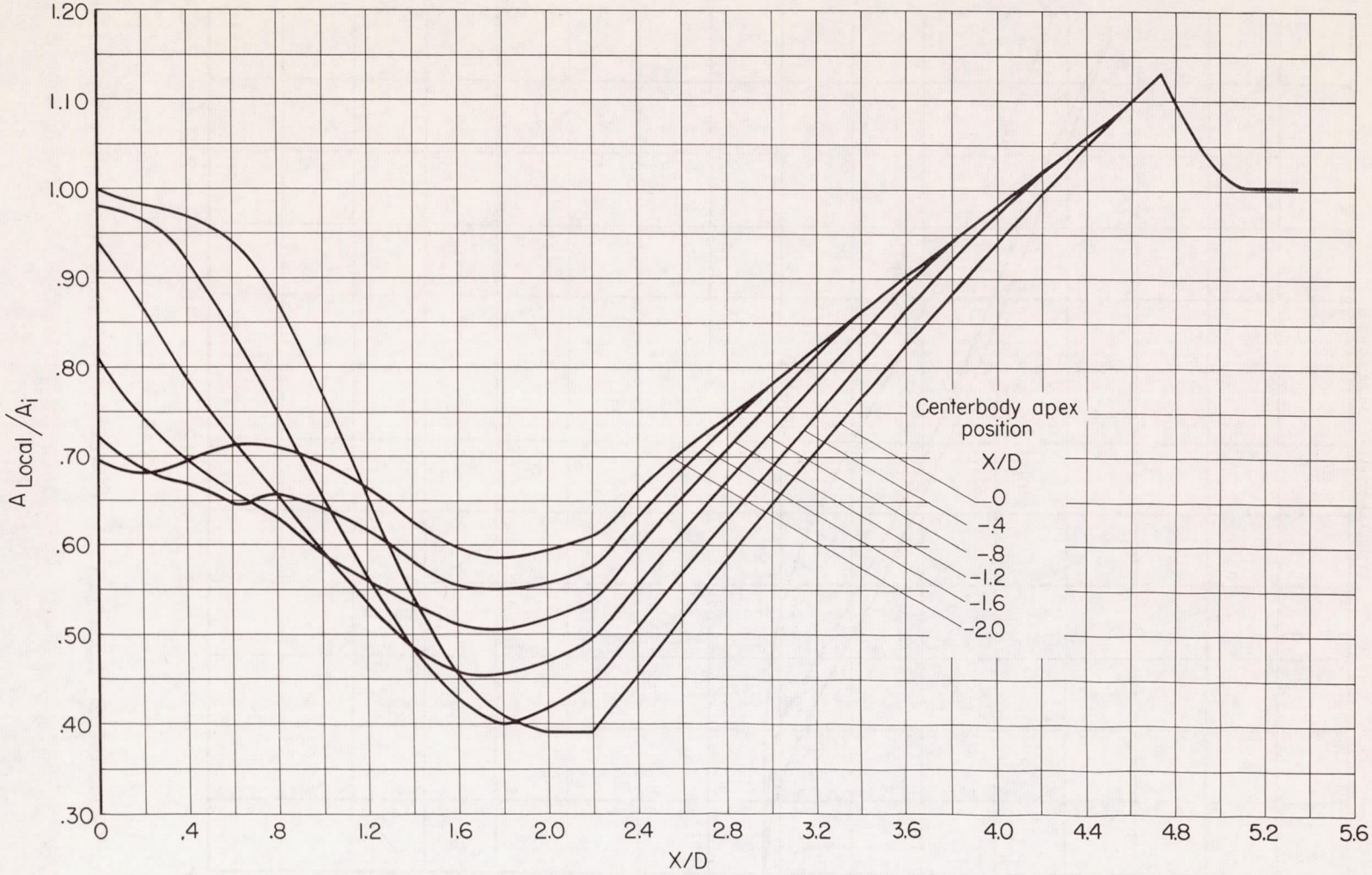
(a) Inlet I

Figure 3.- Longitudinal area distribution.



(b) Inlet 2

Figure 3.- Continued.



(c) Inlet 3

Figure 3.- Concluded.

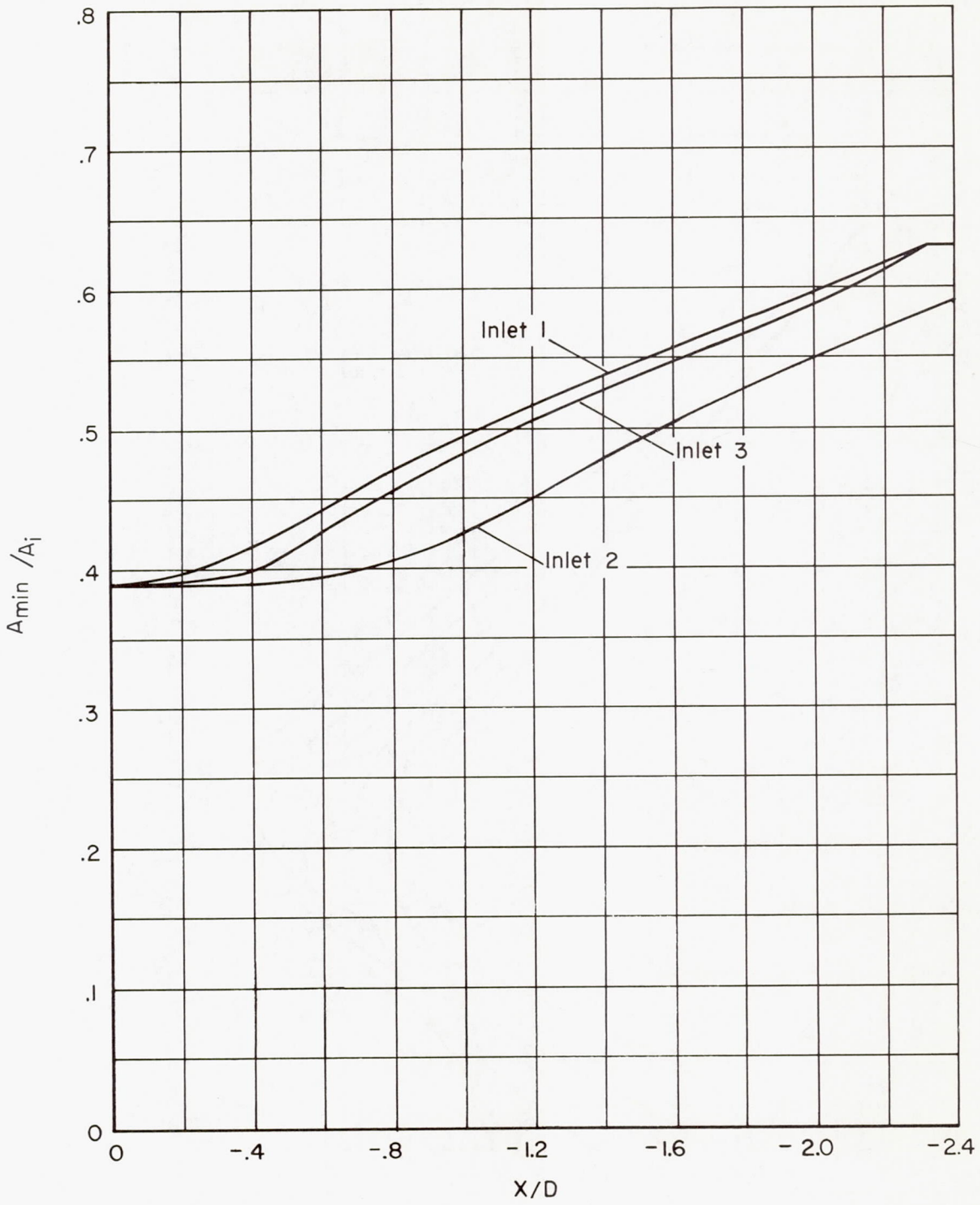
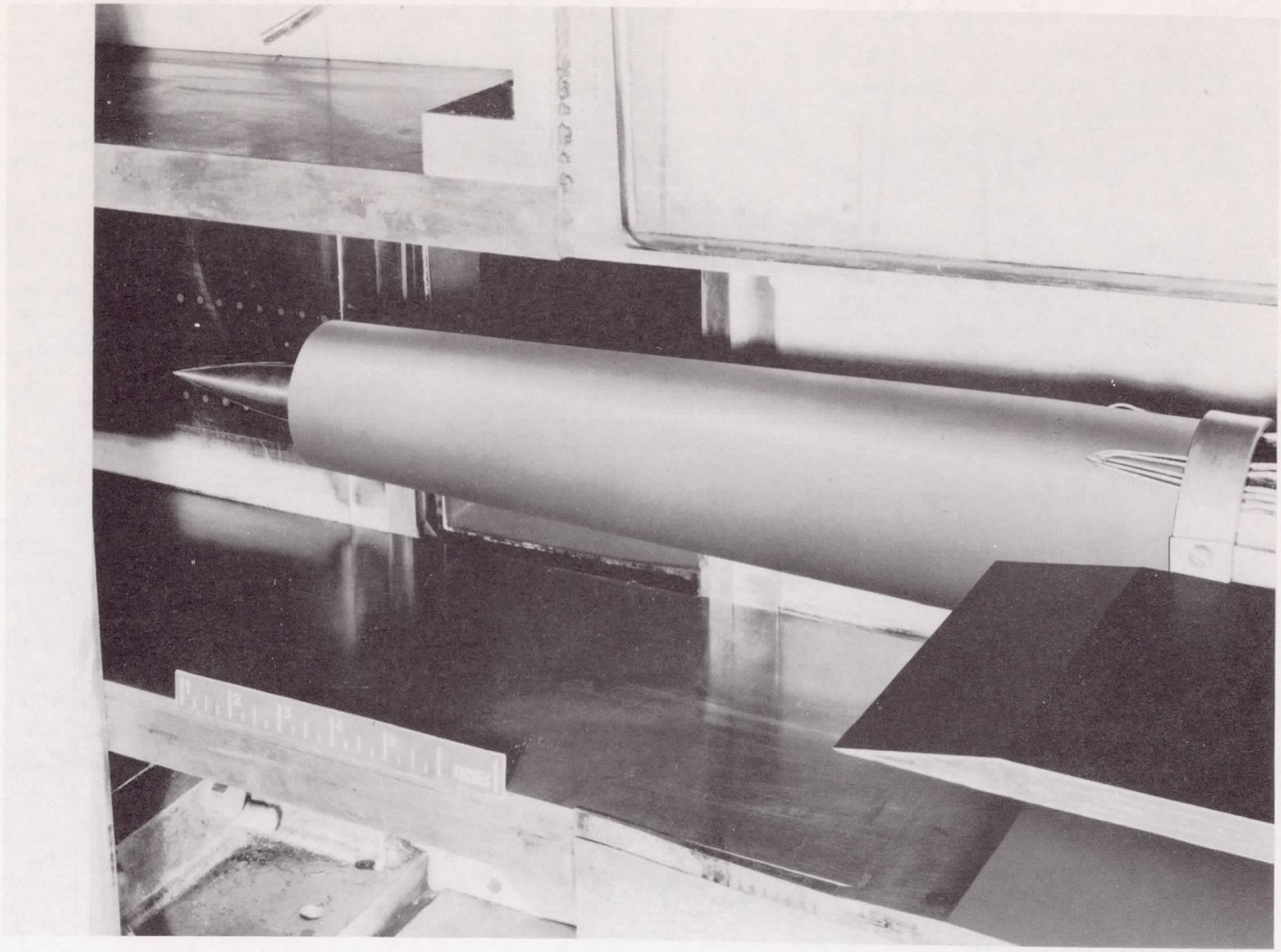


Figure 4.- Variation of contraction ratio with centerbody apex position.



A-20675.1

Figure 5.- Photograph of a circular internal-compression inlet mounted in the wind tunnel.

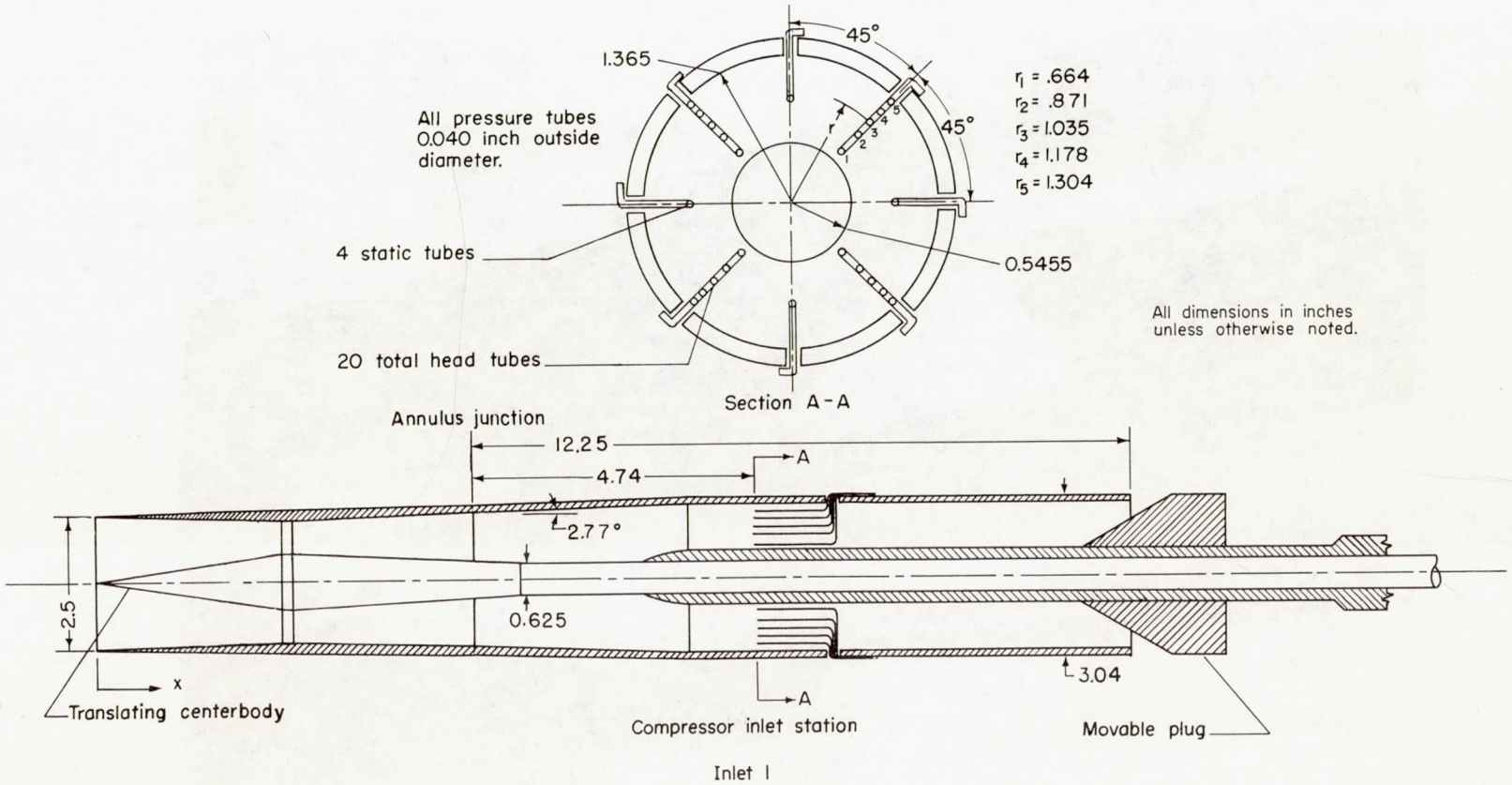


Figure 6.- Sketch of the air-induction model.

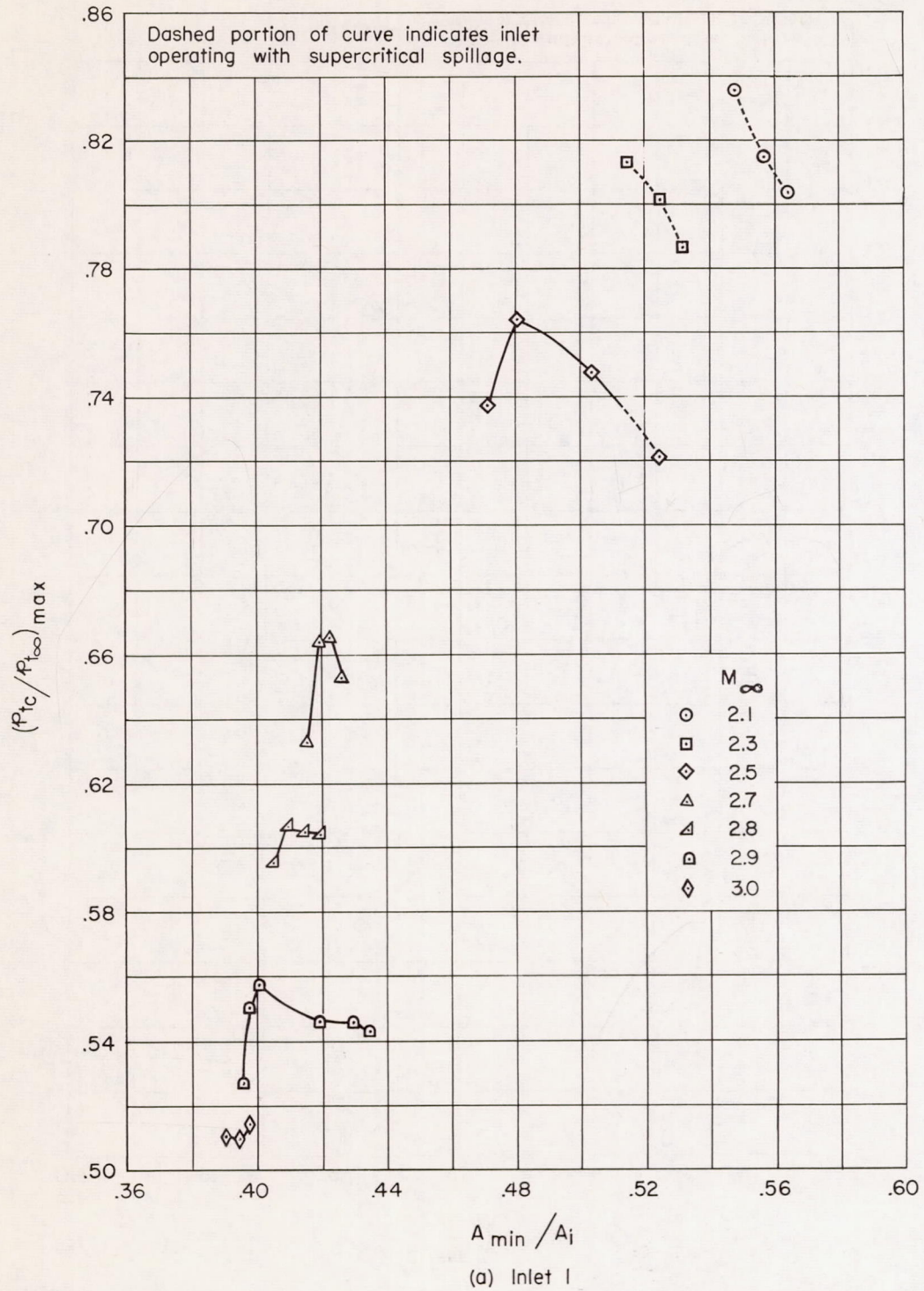
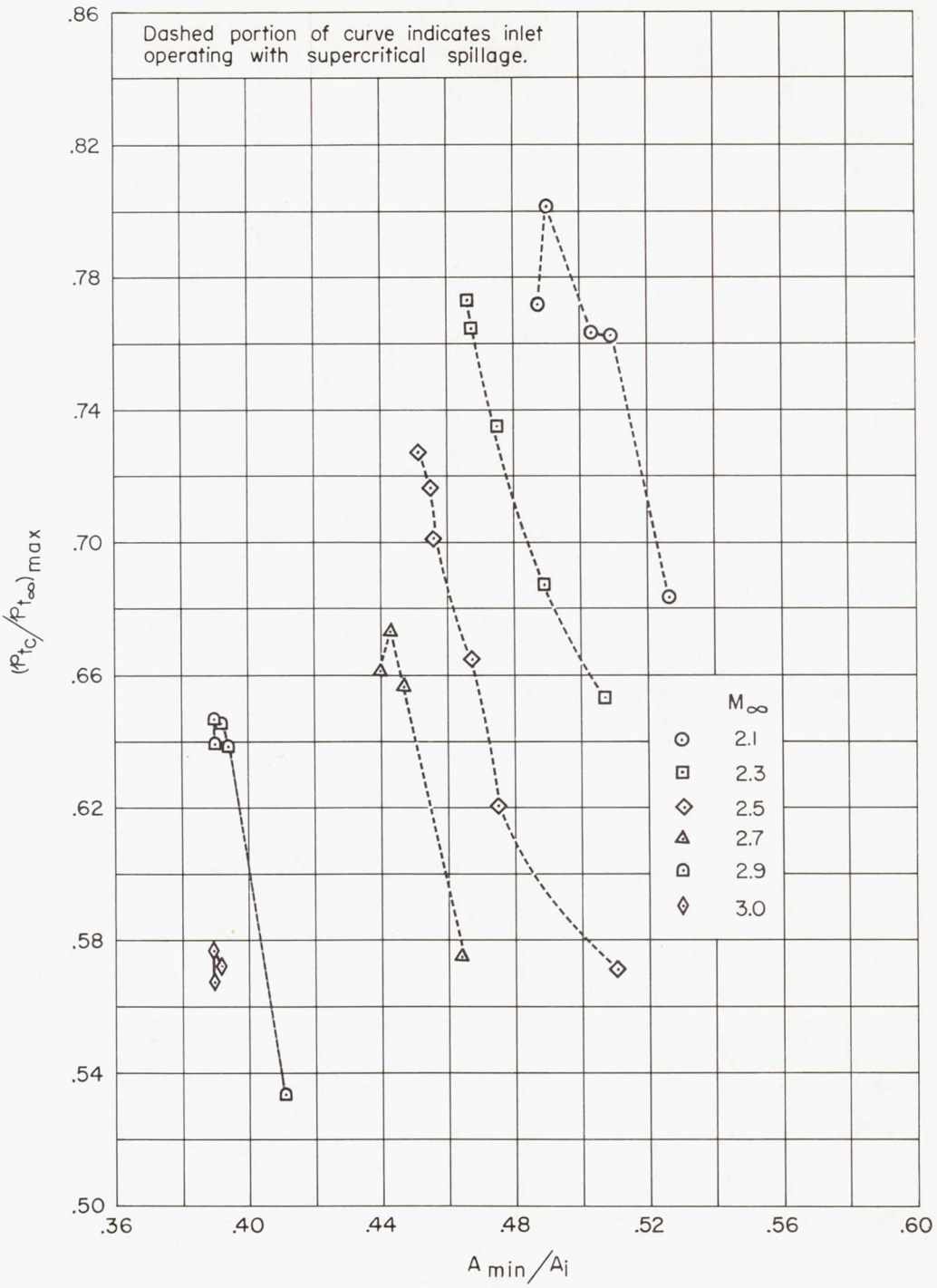
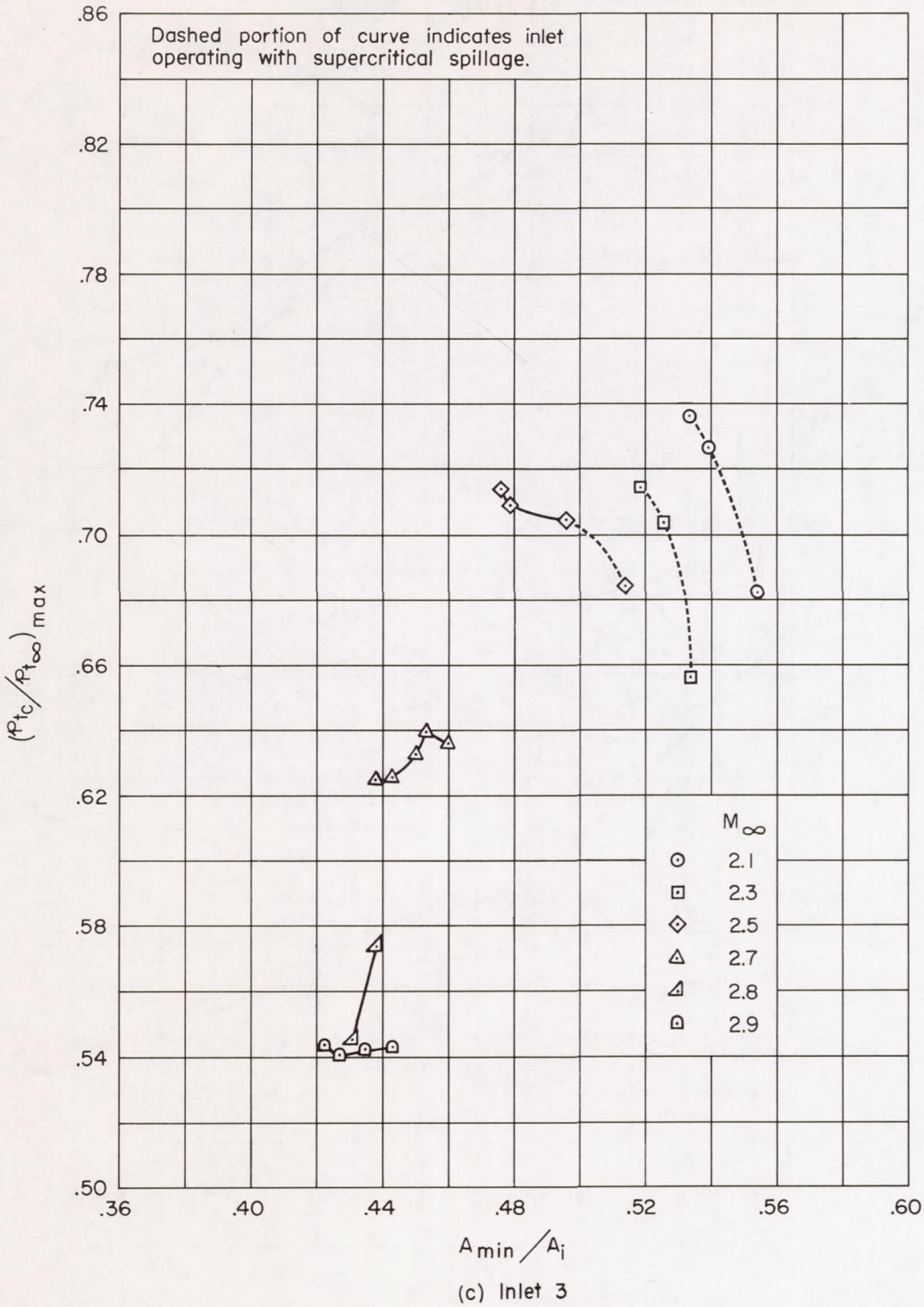


Figure 7.- Pressure recovery as a function of the contraction ratio for the circular internal-compression inlets.



(b) Inlet 2

Figure 7.- Continued.



(c) Inlet 3

Figure 7.- Concluded.

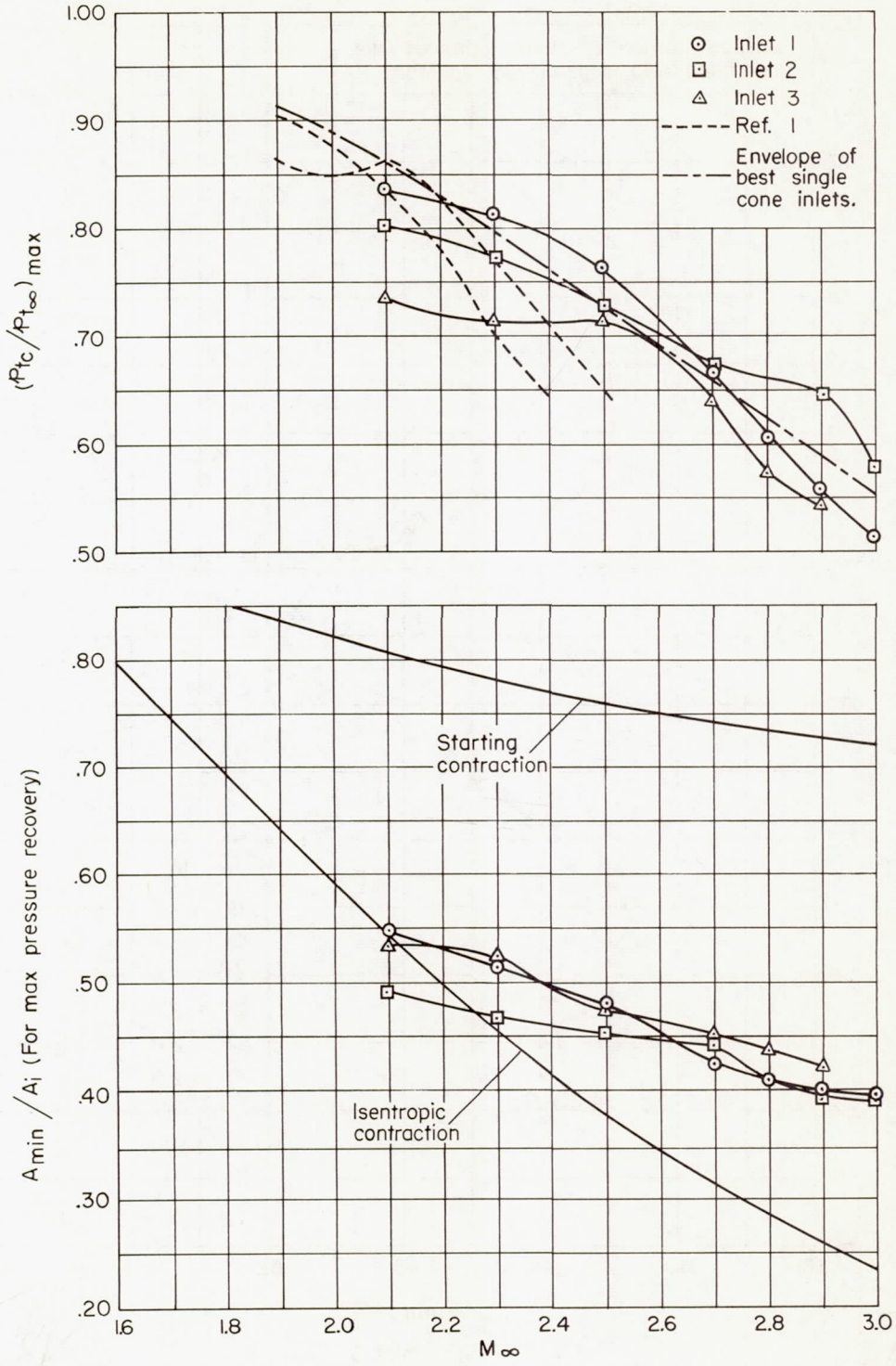
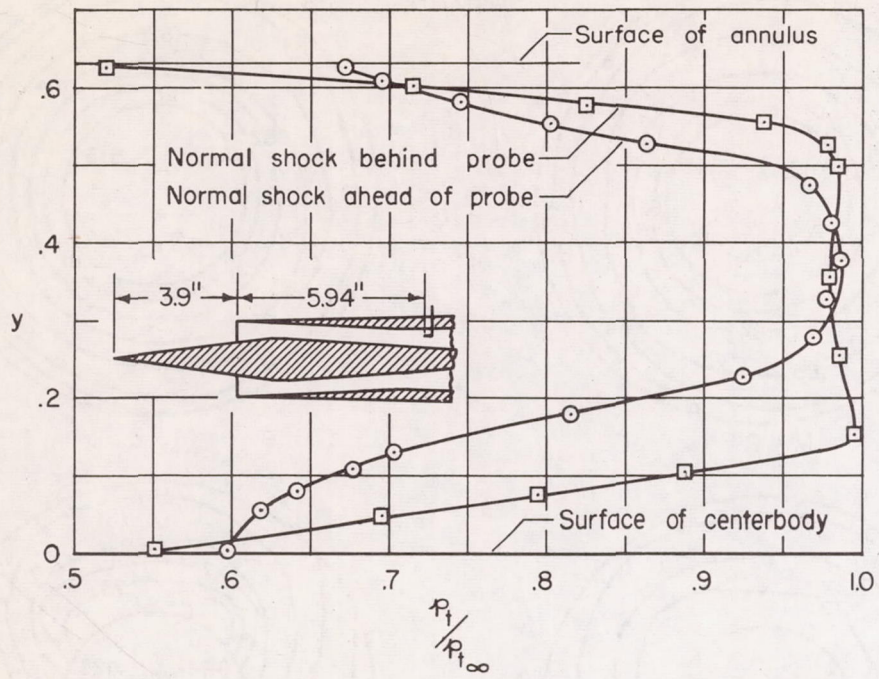
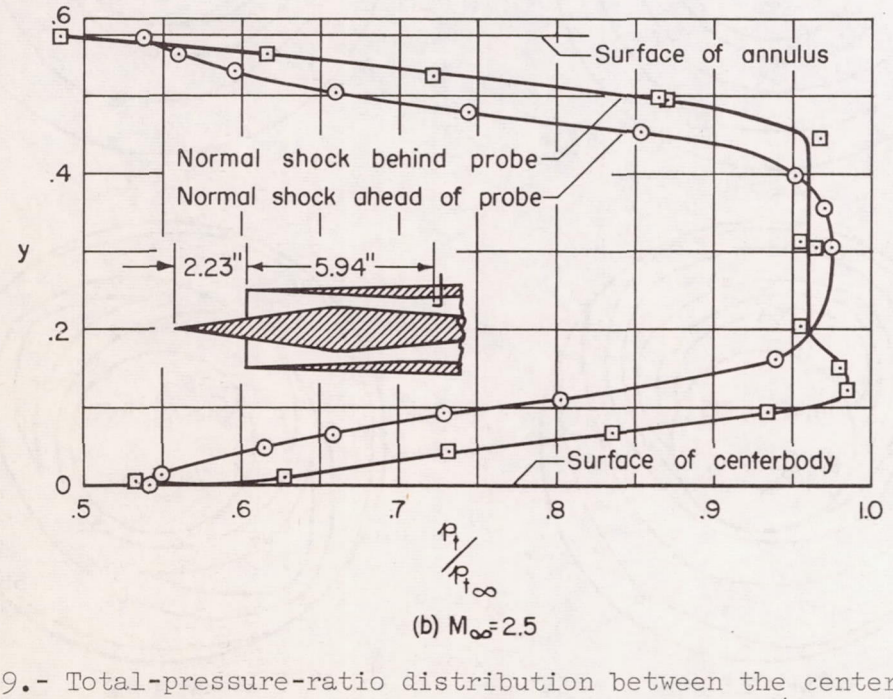


Figure 8.- Maximum pressure recovery and the corresponding contraction ratio as a function of Mach number.



(a) $M_\infty = 2.1$



(b) $M_\infty = 2.5$

Figure 9.- Total-pressure-ratio distribution between the centerbody and annulus surfaces of inlet 1. Centerbody position, X/D, near position for maximum pressure recovery.

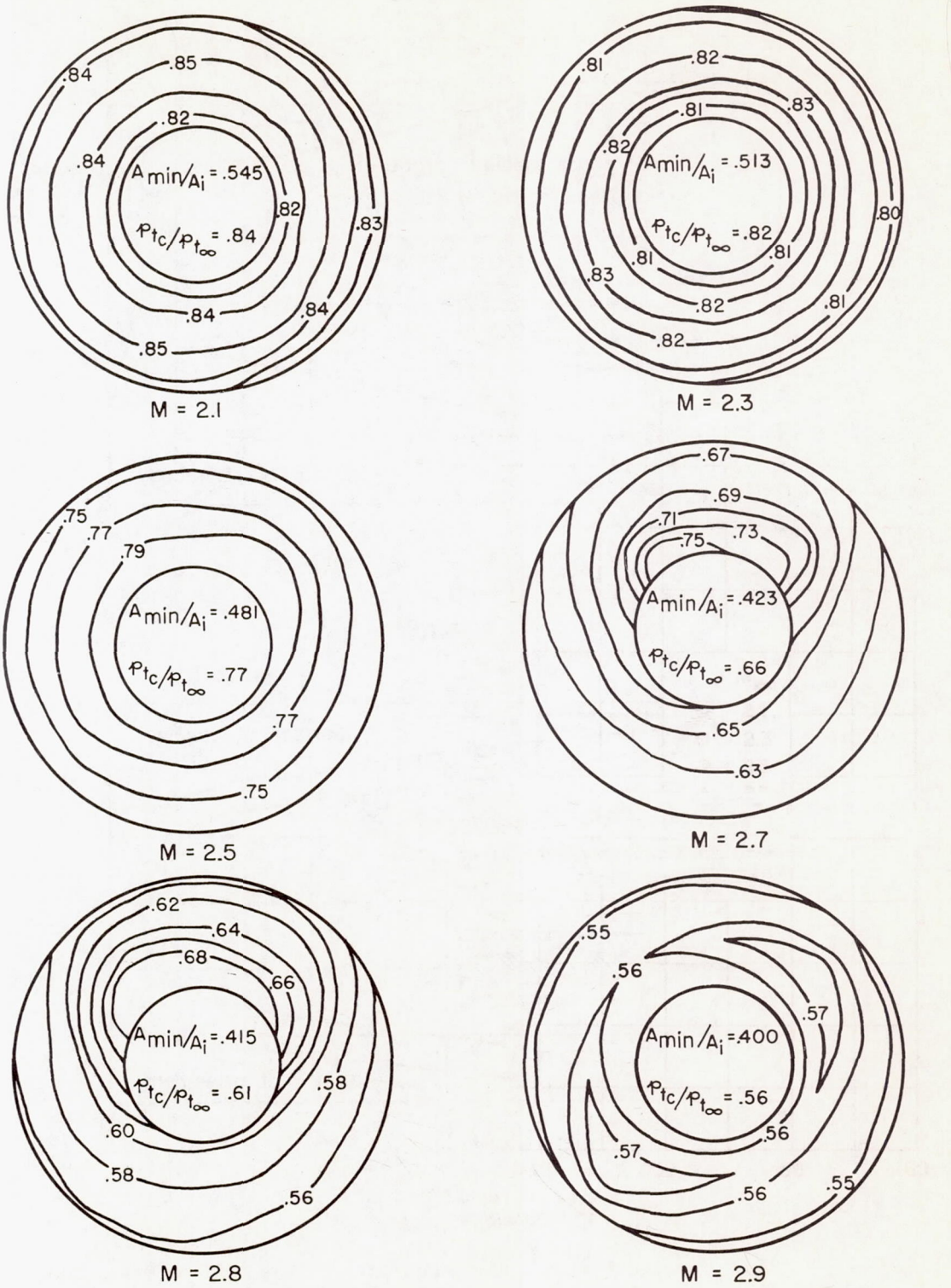


Figure 10.- Total-pressure-ratio contour maps at the compressor station for inlet 1.